Computational Blood Flow Behaviour for Two Rheological Models

M. A. A. Bortoloti
Laboratório Nacional de Computação Científica
Av Getúlio Vargas, 333, Quitandinha, 25651-070, Petrópolis-RJ, Brasil
marciob@lncc.br

J. Karam F.
Laboratório Nacional de Computação Científica
Av Getúlio Vargas, 333, Quitandinha, 25651-070, Petrópolis-RJ, Brasil
jkfi@lncc.br

Abstract. *In this work, blood flow behaviours in meso and micro circulation are investigated in the computational rheology context. Two constitutive equations are investigated for medium and small vessel geometry. One of them is based on the Power Law relation in which pseudoplasticity is entirely supported as a function of the shear rate and the other one is based on the Sisko model that imposes a linear viscosity to a non linear effect. A stabilized finite element method in velocity and discontinuous pressure is generalised for the non linear problems involved here. Hematocrit effects are included besides the shear rate dependence.*

Keywords:*Blood Flow, Pseudoplastic Flow, Finite Element Method, Power Law Relation, Sisko Relation*

1. Introduction

Blood is a special fluid which behaves differently depending on where it is flowing in. These differences come out depending on several factors, being very evident if blood is flowing in large or in small vessels. These vessel hierarchy are traditionally called macro (arteries) and microcirculation (capillary) respectively. From the non-newtonian fluid mechanics point of view there is a region between those two extremes where transition from Newtonian (large vessels) to non-Newtonian behaviour occurs. This region is called here as mesocirculation .

Blood is very known to be a suspension of cells in a nearly newtonian fluid called plasma with major part of the suspension in number being the red blood cell ($\sim 95\%$); and the aggregative phenomenon that happens at low shear rate combined with the rate of red cells to whole blood (hematocrit) are two important factors to produce blood non-Newtonian behaviours.

Several constitutive equations have been proposed to describe the non-Newtonian behaviour of blood and experiments supply the constitutive parameters from viscometric flows.

In order to investigate the flow characterization of two of those constitutive equations when they are applied to non viscometric flows, in this work computational experiments are performed for stenosed vessels in meso-micro circulation to a Power Law relation compared with s Sisko-like model. Viscometric data have been used from the measurements of Wang and Stoltz(1994a) and for the Sisko relation we propose a third order least-square curve fitting to adjust the hematocrit property functions besides the dependence of the shear rate.

Computational results are obtained by a stabilized finite element method in continuous velocity and discontinuous pressure interpolations that was proposed in Bortoloti and Karam (2004), which generalizes the formulation of Karam and Loula (1992), for non linear problems, allowing equal interpolation orders.

2. Mathematical Model

The mathematical description of the stationary incompressible blood flow at low Reynolds numbers can be given by the momentum and the continuity equations

$$-\operatorname{div}\tau = \mathbf{f} \tag{1}$$

$$\operatorname{div}\mathbf{u} = 0 \tag{2}$$

where $\tau = -p\mathbf{I} + \sigma$, p is the hydrostatic pressure, $\mathbf{I}$ is the identity tensor, σ is the shear rate tensor, $\mathbf{f}$ denotes the body forces and $\mathbf{u}$ is the velocity field.

In this work, computational characterization of blood flow is investigated by comparing the Power Law with a Sisko-like model, considering the suspension rate influence.

2.1 Power Law Model

The Power Law relation is one of the most used to model the pseudoplastic behavior. It has good properties from the mathematical point of view, and in some cases it is possible to obtain analytical solutions. Although some complications appear when classical numerical methods are used. To include the hematocrit effect on the apparent viscosity of blood, the Power Law can be written as

$$\sigma = k(H)|\epsilon(\mathbf{u})|^{n(H)-1}\epsilon(\mathbf{u}) \tag{3}$$

in which both the consistence parameters and the power index are functions of the suspension rate. These dependence functions are considered here in view of data from Wang and Stoltz (1994b) as

$$\begin{aligned} k(H) &= 8.29 - 63.11H + 195.5H^2 && (4)\\ n(H) &= 1.262 - 1.833H + 1.297H^2. && (5) \end{aligned}$$

2.2 Sisko Model

The Sisko-like model that is considered here was proposed in Wang and Stoltz (1994a) and it presents a combination between the Newtonian and the Power Law relation as

$$\sigma = \eta_p(\eta(H) + \beta(H)|\epsilon(\mathbf{u})|^{-1/2})\epsilon(\mathbf{u}) \tag{6}$$

where η_p is the newtonian plasma viscosity, $\eta(H)$ and $\alpha(H)$ are two non-dimensional function parameters. For these two functions, using the measured data from Wang and Stoltz (1994a), we propose the following hematocrit dependence:

$$\begin{aligned} \eta(H) &= 110.1682H^3 - 118.2668H^2 + 43.0424H - 2.9333 && (7)\\ \beta(H) &= -355.0794H^3 + 489.3956H^2 - 147.9375H + 13.5196 && (8) \end{aligned}$$

Considering the equations (1) and (2), we have the following Dirichlet boundary value problem

$$\begin{aligned} -\mathrm{div}\,(\mu(\mathbf{u})\epsilon(\mathbf{u})) + \nabla p &= \mathbf{f} \text{ in } \Omega\\ \mathrm{div}\,\mathbf{u} &= 0 \text{ in } \Omega\\ \mathbf{u} &= \overline{\mathbf{u}} \text{ on } \partial\Omega \end{aligned} \tag{9}$$

with

$$\mu(\mathbf{u}) = \xi_1 + \xi_2|\varepsilon(\mathbf{u})|^{\xi_3 - 1} \tag{10}$$

where, to describe the Power Law behavior we are considering

$$\begin{aligned} \xi_1 &= 0\\ \xi_2 &= k(H)\\ \xi_3 &= n(H) \end{aligned}$$

and to describe the Sisko behavior, we have

$$\begin{aligned} \xi_1 &= \eta_P\eta(H)\\ \xi_2 &= \eta_P\beta(H)\\ \xi_3 &= 1/2. \end{aligned}$$

3. Numerical Solution Methodology

By generalizing the formulation of Karam and Loula (1992), here Problem 9 is solved by the following Petrov-Galerkin finite element method.

Let $\Omega \subset \mathbb{R}^2$ be a boundary set discretized by the classical uniform mesh of finite elements with N_e elements. The approximation spaces to velocity and pressure are constructed considering the pressure field as $p_h = p_h^* + \overline{p}_h$, where $p_h^* \in \mathbf{V_h}$ and $\overline{p}_h \in \overline{\mathbf{W}}_\mathbf{h}$ defined as follow

$$\mathbf{V_h} = (S_h^k \cap W_0^{1,2}(\Omega))^2$$

$$\mathbf{W_h^*} = \{p_h^* \in Q_h^l \cap L_0^2(\Omega),\ \nabla p_h^e = \nabla p_h^*\}$$

$$\overline{\mathbf{W}}_\mathbf{h} = \{\overline{p}_h \in Q_h^l \cap L^2(\Omega);\ \nabla \overline{p}_h^e = 0,\ \overline{p}_h^e = \int_{\Omega^e} p_h^e d\Omega^e / \int_{\Omega^e} d\Omega^e\}$$

where S_h^k is the continuous Lagrangean polynomial set of degree k, Q_h^l is the discontinuous Lagrangean polynomial set of degree l and p_h^e and $\overline{p}_h^e$ are the Ω^e-constraints of p_h and $\overline{p}_h$ respectively. Therefore the variational form is

Problem PG$_{hd}$: Given $\mathbf{f} \in \mathbf{V_h'}$, the dual space of $\mathbf{V_h}$, find $\{\mathbf{u_h}, p_h^*, \overline{p}_h\} \in \mathbf{V_h} \times \mathbf{W_h^*} \times \overline{\mathbf{W}}_\mathbf{h}$, such that

$$(A_h^*(U_h^*); V_h^*) + B_h(\overline{p}_h, \mathbf{v_h}) = F_h^*(V_h^*) \quad \forall \quad \{\mathbf{v_h}, q_h^*\} \in \mathbf{V_h} \times \mathbf{W_h^*}$$

$$B_h(\overline{q}_h, \mathbf{u_h}) = 0 \quad \forall \quad \overline{q}_h \in \overline{\mathbf{W}}_\mathbf{h}$$

where

$$(A_h^*(U_h^*); V_h^*) = (\mu(\mathbf{u_h})\varepsilon(\mathbf{u_h}), \varepsilon(\mathbf{v_h})) + B_h(p_h^*, \mathbf{v_h}) + \delta_2\vartheta(\mathrm{div}\,\mathbf{u_h}, \mathrm{div}\,\mathbf{v_h})$$

$$+B_h(q_h^*, \mathbf{u_h}) + \frac{\delta_1 h^2}{\vartheta}(-\Delta_\mu \mathbf{u_h} + \nabla p_h^*; -\Delta_\mu \mathbf{v_h} + \nabla q_h^*)_h \tag{11}$$

$$B_h(p_h^*, \mathbf{v_h}) = -(p_h^*, \mathrm{div}\,\mathbf{v_h}) \tag{12}$$

$$F_h^*(V_h^*) = \mathbf{f}(\mathbf{v_h}) + \frac{\delta_1 h^2}{\vartheta}(\mathbf{f}; -\Delta_\mu \mathbf{v_h} + \nabla q_h^*)_h \tag{13}$$

with the apparent viscosity defined in (10), h denoting the mesh parameter, $\mu(\mathbf{u_h}) = |\varepsilon(\mathbf{u_h})|^{\alpha-2}$, $(u,v) = \int_\Omega u\, v\, d\Omega$, $(u,v)_h = \sum_{e=1}^{N_e} \int_{\Omega^e} u\, v\, d\Omega^e$, δ_1 and δ_2 being positive constants denominated as stability parameters, ϑ being a dimensional parameter, $\Delta_\mu \mathbf{u_h} = \mathrm{div}\,(\mu(\mathbf{u_h})\varepsilon(\mathbf{u_h}))$, $U_h = \{u_h, p_h\}$, $U_h^* = \{u_h, p_h^*\}$, $\overline{U}_h = \{u_h, \overline{p}_h\}$ and N_e being the number of elements.

This formulation allows the use of same order interpolation functions for the velocity and the pressure by satisfying the following relation between the stabilizing parameters:

$$\frac{(\gamma\xi_2 + \xi_1)\delta_1\gamma_P}{\vartheta(\gamma\xi_2 + \xi_1) + \delta_1(r_2 + C_l)} - \frac{1}{\delta_2\vartheta} > 0$$

where the other constants come from the mathematical requirements, for example coercivity and continuity of the $(A_h^*(U_h^*), V_h^*)$ and $B_h(p, \mathbf{u_h})$ forms.

The nonlinear problem generated by the constitutive equation is solved by the following algorithm of Uzawa type:

PG$_{hd}^n$**Problem**: Given u_h^0 and p_h^0, find $\{u_h^n, p_h^{*n}, \overline{p}_h^n\} \in \mathbf{V_h} \times \mathbf{W_h^*} \times \overline{\mathbf{W}}_\mathbf{h}$, $n > 0$, such that

$$(\mu(\mathbf{u_h^n})\varepsilon(\mathbf{u_h^{n+1}}), \varepsilon(\mathbf{v_h})) + B_h(p_h^{n+1}, \mathbf{v_h}) + B_h(q_h, \mathbf{u_h^{n+1}}) + \delta_2\vartheta(\mathrm{div}\,\mathbf{u_h^{n+1}}, \mathrm{div}\,\mathbf{v_h})$$

$$+\frac{\delta_1 h^2}{\vartheta}(-\mathrm{div}\,(\mu(\mathbf{u_h^n})\varepsilon(\mathbf{u_h^{n+1}})) + \nabla p_h^{*n+1}, -\mathrm{div}\,(\mu(\mathbf{v_h})\varepsilon(\mathbf{v_h})) + \nabla q_h)_h = F_h^*(V_h^*)$$

$$\forall \quad \{\mathbf{v_h}, q_h^*, \overline{q}_h\} \in \mathbf{V_h} \times \mathbf{W_h^*} \times \overline{\mathbf{W}}_\mathbf{h} \tag{14}$$

$$\mathbf{u_h}^{n+1} = \mathbf{u_h}^n + \rho_n \nabla p_h^n \quad \text{where} \quad \rho_n > 0. \tag{15}$$

Existence and uniqueness of solution are achieved for

$$0 < \rho < \frac{2(\gamma\xi_1 + \xi_2)(1-\chi)}{C_l^2 + C^2}$$

with $1/2 < \chi < 1$.

4. Computational Rheological Characterization Experiments

Numerical experiments have been performed for stenosed vessels whose meshes are illustrated in Fig. 1, for different dimensions: small vessels with $d_1 = 0.05mm$, $d_2 = 0.5mm$ and medium vessels with $d_1 = 1mm$, $d_2 = 10mm$. Meshes have been constructed with 4141 nodes and 1000 biquadratic elements. 40% and 60% Hematocrit have been considered. For the large vessel it was prescribed an inlet velocity of $10mm/s$ and for the smaller one a $0.5mm/s$ velocity has been imposed. Results may be observed from Fig 2-9 in terms of velocity norm, pressure norm, stress tensor norm and apparent viscosity.

From the results, for small vessels with hematocrit of 40% (low concentration) power-law and Sisko are nearly equivalent, with Sisko giving a little greater apparent viscosity at the center of the straight part of the vessel and a larger strip of low viscosity to the wall. In the core of the stenose, power-law gives a little greater viscosity and at the wall they are almost equivalent. This is reflected in the subtle differences to the velocity, stress and pressure results in sub-figures (a) and (b) of Figs. 2-5.

Increasing the hematocrit to 60% increases the differences between the results for the two models. It can be seen from the velocity graphics of Figs. (2c) and (2d) that the power-law model causes the velocity field more flat than the Sisko one. The corresponding apparent viscosity graphics in Figs. (5c) and (5d) confirm this. It can be seen, from Figs. (3c) and (3d), that in the stenose the pressures obtained with the power-law model are greater than those obtained with the Sisko relation. From Figs. (4c) and (4d) it is possible to observe that the stresses at the wall of the stenose are bigger from the Sisko model.

For medium vessels, when the hematocrit is 40%, few differences are observed between the models, but a subtle larger viscosity is obtained for the Sisko model from Fig (9b) when compared with Fig. (9a) for power-law, reflecting also in subtle differences in the other corresponding results, sub-figures (a) and (b) of Figs. (6-9).

Increasing the hematocrit to 60% it also increases the differences between the results for the two models. It can be seen from sub-figures (c) and (d) of Figs. (6-9). these differences are more pronounced than the differences obtained with hematocrit 40% in the straight part of the vessel, which is larger than the stenose.

For 60% hematocrit, power-law shear stresses are bigger at the entrance and at the exit of the stenose and it is the opposite in the middle way region. For small vessels power-law is more pseudoplastic than Sisko inside the stenose and for medium vessels Sisko is more newtonian at the beginning and at the end of the stenose, that is in the larger diameter part of the vessel, where more newtonian behaviour is expected. A better understanding of this aspect can be seen from Fig. 10. Fig. (10a) depicts the velocity profiles for the small vessel at $d_2/4$, straight anterior part, showing that there are few differences between the models in this case. Fig. (10b) depicts the velocity profiles for the medium vessel at $d_2/4$, showing that (and it is more pronounced for hematocrit 60%) power-law model tends to overestimate pseudoplasticity and Sisko relation, even capturing the shear thinning, gives results between the pure pseudoplastic and the Newtonian result. The Newtonian result is the one expected when diameter goes from medium to large. Then, it suggests that Sisko is more able to capture the expected variations inside the range going from pseudoplastic to Newtonian behaviours.

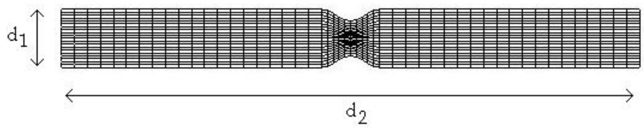

Figure 1. Stenotic mesh

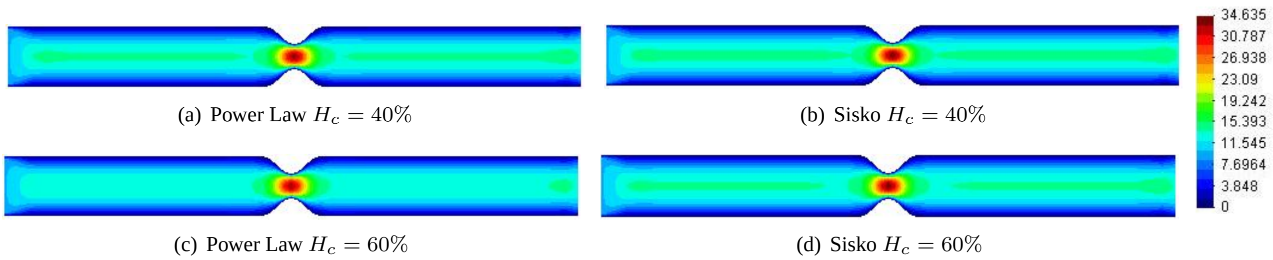

(a) Power Law $H_c = 40\%$ (b) Sisko $H_c = 40\%$

(c) Power Law $H_c = 60\%$ (d) Sisko $H_c = 60\%$

Figure 2. Velocity norm to small vessel

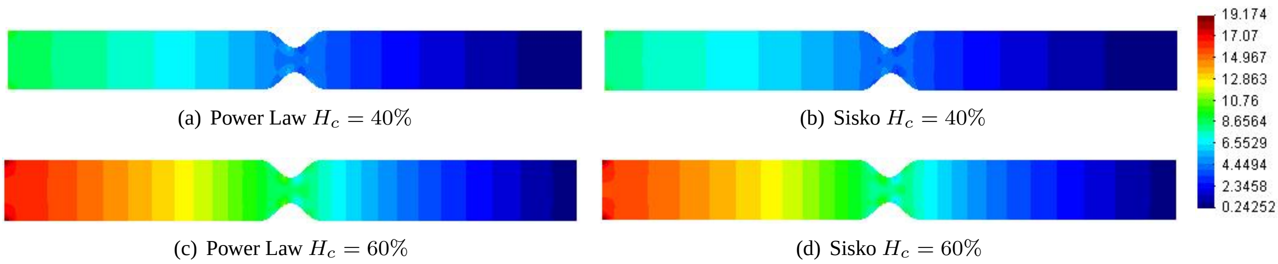

(a) Power Law $H_c = 40\%$ (b) Sisko $H_c = 40\%$

(c) Power Law $H_c = 60\%$ (d) Sisko $H_c = 60\%$

Figure 3. Pressure norm to small vessel

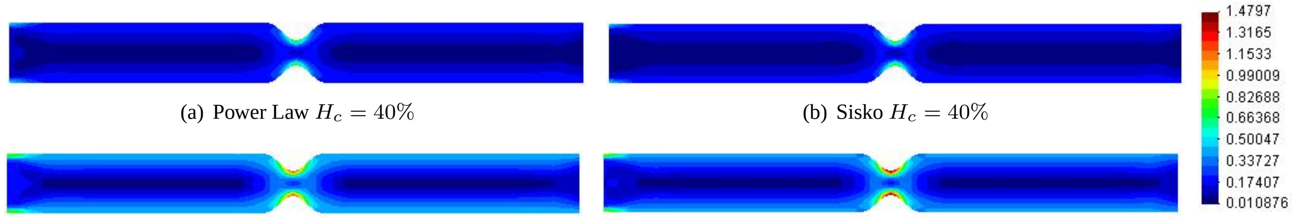

(a) Power Law $H_c = 40\%$ (b) Sisko $H_c = 40\%$

(c) Power Law $H_c = 60\%$ (d) Sisko $H_c = 60\%$

Figure 4. Stress tensor norm to small vessel

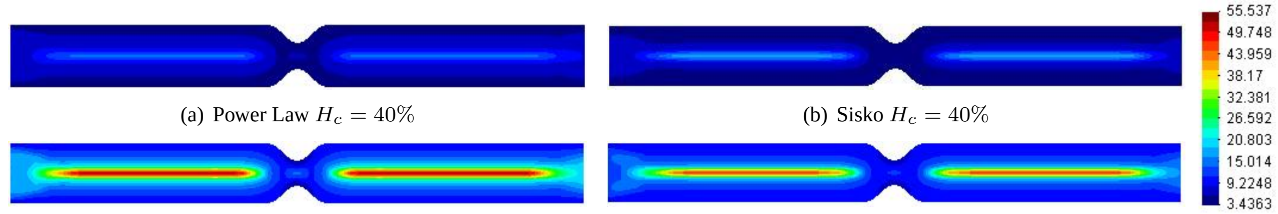

(a) Power Law $H_c = 40\%$ (b) Sisko $H_c = 40\%$

(c) Power Law $H_c = 60\%$ (d) Sisko $H_c = 60\%$

Figure 5. Apparent viscosity to small vessel

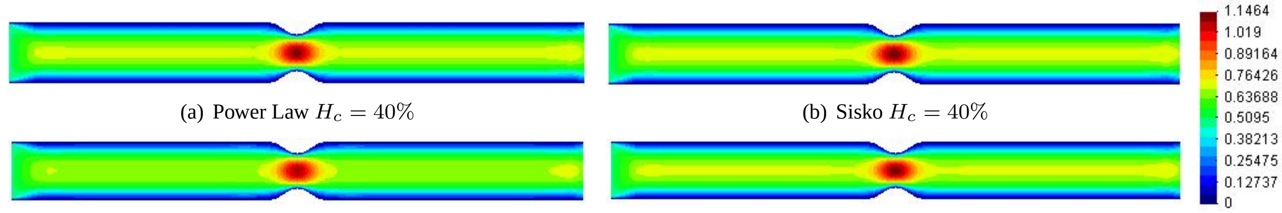

(a) Power Law $H_c = 40\%$ (b) Sisko $H_c = 40\%$

(c) Power Law $H_c = 60\%$ (d) Sisko $H_c = 60\%$

Figure 6. Velocity norm to medium vessel

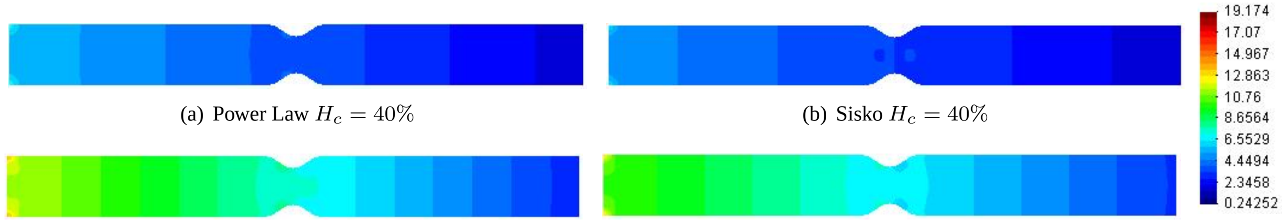

(a) Power Law $H_c = 40\%$ (b) Sisko $H_c = 40\%$

(c) Power Law $H_c = 60\%$ (d) Sisko $H_c = 60\%$

Figure 7. Pressure norm to medium vessel

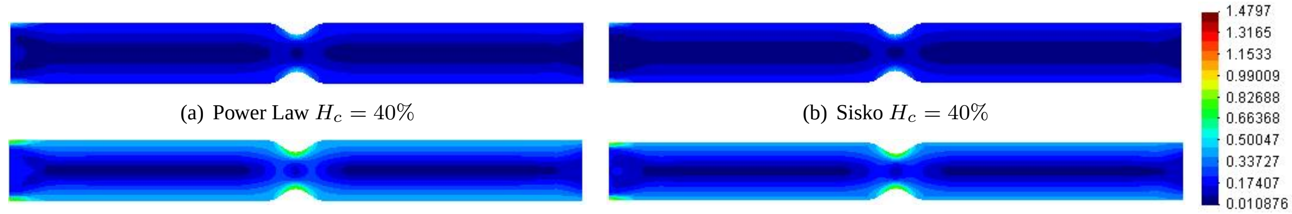

(a) Power Law $H_c = 40\%$ (b) Sisko $H_c = 40\%$

(c) Power Law $H_c = 60\%$ (d) Sisko $H_c = 60\%$

Figure 8. Stress tensor norm to medium vessel

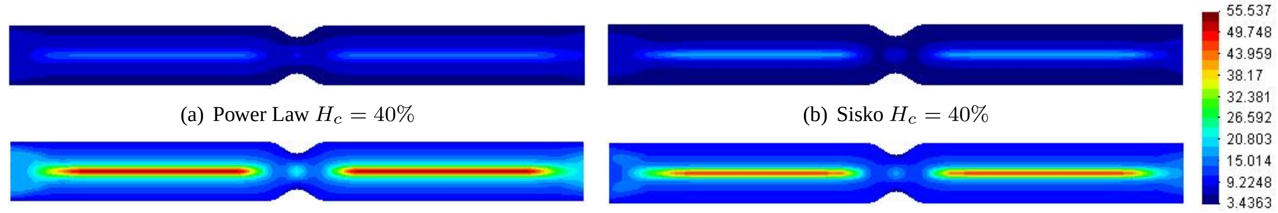

(a) Power Law $H_c = 40\%$ (b) Sisko $H_c = 40\%$

(c) Power Law $H_c = 60\%$ (d) Sisko $H_c = 60\%$

Figure 9. Apparent viscosity to medium vessel

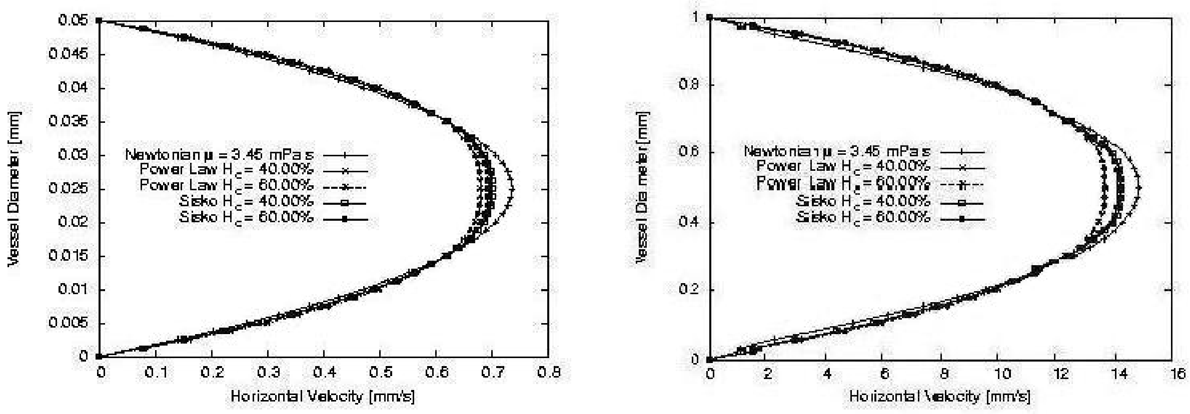

(a) Small vessel (b) Medium vessel

Figure 10. Velocity profiles at d2/4

5. Conclusions and Remarks

In this work, some differences between Power law and Sisko models have been analyzed, considering the dependence of the viscosity with hematocrit besides the shear rate for blood flow in the mesocirculation for stenosed vessel and for hematocrit of 40% and 60% .

In the case of the Sisko model, we proposed a third order least-square curve fitting. A stabilized mixed finite element method in velocity and discontinuous pressure has been used.

This formulation allows equal order interpolations for velocity and pressure being more accurate than when continuous interpolations are used, especially for critical boundary conditions.

The numerical results obtained reveal different flow patterns when power law and Sisko are considered with Hematocrit and shear rate playing an important game.

Sisko model presented more ability in capturing pseudoplasticity and tendency to Newtonian behaviour when going from small to medium vessels.

6. Acknowledgements

M. A. A. Bortoloti would like to acknowledge CAPES/BR for his graduate grant.

J. Karam F. would like to acknowledge PRONEX/FAPERJ project no. E-26/171.199/2003.

7. References

Bortoloti, M. A. A. and Karam F., J., 2004, "Equal-Order v-p Stabilized Finite Element Methods for Pseudoplasticity", Proceedings of Second Brazilian Conference on Rheology, Rio de Janeiro, Brazil pp 73-74.

J. Karam F. and A. F. D. Loula, , 1992, "On Stable Equal-Order Finite Element Formulations for Incompressible Flow Problems", International Journal for Numerical Methods in Engineering, Vol. 34, no. 2, pp. 655-665.

Wang, I., Stoltz, J. F., 1994a, "Characterization of pathological bloods with a new rheological relationship", Clinical Hemorheology, Vol. 14, No. 2, pp. 237-244.

Wang, I. and Stoltz, J. F., "Influence of nonnewtoninan properties of blood on the global transport of red blood cells", Clinical Hemorheology, Vol. 14, No. 6, pp. 789-796, 1994b.

8. Responsibility notice

The author(s) is (are) the only responsible for the printed material included in this paper